



Surface and finite-size effects on N –Sm-A–Sm-C phase transitions in free-standing filmsE. J. L. de Oliveira ¹, D. C. S. de Melo,¹ Maria S. S. Pereira,¹ L. R. Evangelista,² and I. N. de Oliveira ¹¹*Instituto de Física, Universidade Federal de Alagoas 57072-970 Maceió-AL, Brazil*²*Departamento de Física, Universidade Estadual de Maringá 87020-900 Maringá-PR, Brazil*

(Received 19 June 2020; accepted 3 August 2020; published 19 August 2020)

The present study is devoted to the investigation of surface anchoring and finite-size effects on nematic–smectic-A–smectic-C (N –Sm-A–Sm-C) phase transitions in free-standing films. Using an extended version of the molecular theory for smectic-C liquid crystals, we analyze how surface anchoring and film thickness affect the thermal behavior of the order parameters in free-standing smectic films. In particular, we determine how the transition temperature depends on the surface ordering and film thickness. We show that the additional orientational order imposed by the surface anchoring may lead to a stabilization of order parameters in central layers, thus modifying the nature of the phase transitions. We compare our results with experimental findings for typical thermotropic compounds presenting a N –Sm-A–Sm-C phase sequence.

DOI: [10.1103/PhysRevE.102.022702](https://doi.org/10.1103/PhysRevE.102.022702)**I. INTRODUCTION**

The comprehension of phase transitions involving smectic liquid crystals is a long standing issue. In these systems, a very rich phenomenology can be observed due to the interplay of anisotropic critical behavior [1,2], surface ordering [3–5], finite-size effects [6,7], and external fields [8–10]. In particular, smectic samples have a unique ability of forming freely suspended films, also termed as free-standing films, which correspond to a stack of smectic layers confined in a surrounding gas [11]. Due to the absence of a solid substrate, the equilibrium configuration is determined by the film holder, with the surface tension reducing the thermal fluctuations at the film surface [12]. In fact, surface anchoring conditions at the gas/film interface can lead to the stabilization of the smectic ordering even above the bulk transition temperatures [13]. As a consequence, a large variety of unusual physical phenomena can be observed in free-standing smectic films, such as layer thinning and thickening transitions [14–16], anomalies on the specific heat [2,17,18], thickness dependence of the transition temperature [6], as well as surface-induced biaxiality [5]. Since the film thickness can vary from a few nanometers to several micrometers, free-standing films constitute a suitable experimental setup for understanding how changes in the system dimensionality affect the thermodynamic behavior of the smectic phase [13,19].

Over the past decades, a remarkable amount of interest has been devoted to phase transitions involving smectic liquid crystals with a tilted molecular alignment [2,7,17,18,20–25]. Different experimental techniques have been employed to determine the nature of smectic-C–smectic-A (Sm-C–Sm-A) and smectic-C–nematic (Sm-C–N) phase transitions [17,20–23,26–29]. In rodlike compounds presenting a small or moderate transverse dipole moment ($P \leq 20$ nC/cm²), it has been verified that the Sm-C–Sm-A phase transition has a second-order character [20,22], while the Sm-C–N phase

transition exhibits a first-order behavior with a small latent heat [20]. Moreover, the analysis of heat-capacity measurements in several compounds revealed that the temperature range of the Sm-A phase plays an important role to the behavior of continuous Sm-C–Sm-A phase transition [26], delimiting the crossover between the mean-field tricritical and the ordinary mean-field character of this transition [17]. However, a first-order Sm-C–Sm-A phase transition has been reported in smectogenic compounds presenting a large transverse dipole moment ($P > 50$ nC/cm²) [27], with a large Sm-A temperature range [17]. Besides, a nematic–smectic-A–smectic-C (N –Sm-A–Sm-C) multicritical point has been reported in binary liquid-crystal mixtures [30], as well as in single component systems under high pressures [23].

Motivated by the rich phenomenology observed in the experimental results, several theoretical studies have been performed to better describe transitions involving Sm-C liquid-crystal phase [31–38]. In fact, a large variety of microscopic models have been introduced to characterize intermolecular interactions in smectogenic systems. Assuming a bilinear mean-field potential for the tilt angle distribution, Giebelman and Zugenmeier provided an equation of state for the Sm-C phase [32], consisting in a Langevin function of the reduced tilt angle and the reduced temperature. Despite the good description of the temperature dependence of tilt angle, such an oversimplified model cannot reproduce the variety of experimental phase diagrams. Considering a system of rodlike molecules with a perfect orientational order, van der Meer and Vertogen analyzed how a dipole-induced interaction leads to the emergence of a tilted smectic phase [39], in which the Sm-C–Sm-A transition does not correspond to the usual order-disorder type. Based on molecular interactions between rodlike molecules with off-axis dipoles, Govind and Madhusudana have developed a modified version of McMillan’s model for Sm-A–N-Iso

systems, being successful in the description of experimental phase diagrams presenting the Sm-C phase [33,34]. However, such a model requires the introduction of an excluded-volume contribution to stabilize the Sm-A phase, thus leading to a large number of free parameters. Using a complete set of orientational- and translational-order parameters, recent studies have introduced different pair-interaction potentials for polar and nonpolar molecules, to reproduce phase diagrams containing conventional or “de Vries-type” Sm-C phases [36,37,40–42]. Nevertheless, the use of a complete set of order parameters implies a large number of free parameters in these molecular models, making difficult their comparison with the typical characteristic of liquid-crystalline compounds.

Tilting transitions in free-standing smectic films may exhibit a distinct behavior in relation to those observed in bulk systems [7,21,24,27,43–46]. In fact, surface anchoring conditions and finite size effects tend to affect the thermal behavior of orientational- and translational-order parameters in thin free-standing smectic films. From monitoring the transmittance of such systems close to a second-order Sm-C–Sm-A phase transition, an unusual thickness dependence has been reported for the thermal behavior of the average tilt angle [21], with the transition temperature in thin films being higher than that of a bulk system. Optical ellipsometry measurements have revealed that a finite average tilt may remain in the surface layers of free-standing films, well above the bulk transition temperature [27]. Such a scenario has been supported by electron diffraction measurements in thin film [24], where a surface-induced phase sequence is identified. Moreover, surface-effects may lead to changes in the nature of Sm-C–Sm-A phase transition [27,46], especially in films with a few layers. For compounds presenting a first-order Sm-C–Sm-A bulk phase transition, the discontinuous jump in the tilt angle is replaced by a continuous behavior at the transition temperature, when the film thickness is lower than a characteristic thickness [27,46]. Furthermore, surface anchoring and finite size effects give rise to a nonuniform tilt profile in free-standing Sm-C films [45], with the outermost layers being more tilted than the inner layers. In chiral smectic samples, a series of discrete transitions has been reported [7], where a reentrant synclinic-antclinic-synclinic ordering sequence takes place at the surface film in the presence of an external electric field.

Although several studies have been devoted to the theoretical description of phase transitions in bulk Sm-C systems, microscopic models for free-standing films have not been exploited so far. In the present study, we investigate N –Sm-A–Sm-C phase transitions by using an extended version of the mean-field theory for Sm-C liquid crystals. We analyze how the interplay of surface anchoring and finite size effects affect the thermal behavior of the order parameters in free-standing smectic films. In particular, we show that the additional orientational order imposed by the surface anchoring may lead to a stabilization of order parameters in central layers, thus modifying the nature of the phase transitions. We compare our results with experimental findings for typical thermotropic compounds presenting a N –Sm-A–Sm-C phase sequence.

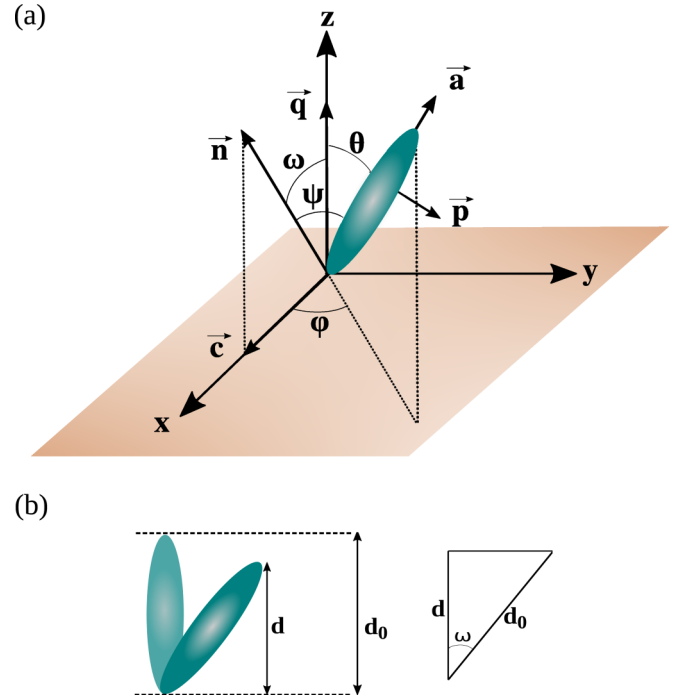


FIG. 1. (a) Schematic representation of the long molecular axis \vec{a} in the Sm-C phase, for a Cartesian coordinate system with the z axis being normal to the smectic layer plane. For convenience, we assume that the director \vec{n} is restricted to the z - x plane, defined as the tilt plane. Here, the vector \vec{c} corresponds to the projection of the director in the x axis, while ω represents the tilt angle of the director \vec{n} in relation to the smectic wave vector \vec{q} . The orientation of the long molecular axis is defined by polar and azimuthal angles θ and ϕ , respectively. ψ is the relative angle between the long molecular axis \vec{a} and director \vec{n} . (b) Representation of the layer contraction induced by the molecular tilt, with d_0 being the layer spacing in the Sm-A phase.

II. MICROSCOPIC MODEL FOR BULK TRANSITIONS

We investigate a single component smectogenic system of rodlike molecules with a small or moderate transverse dipole moment [34], which presents a layer contraction in the tilted smectic phase. To characterize the average molecular orientation inside the smectic layers, we consider the relative orientation of the director \vec{n} ($|\vec{n}| = 1$) and the smectic wave vector \vec{q} , which is represented by average tilt angle ω , as shown in Fig. 1(a), where \vec{q} is assumed to be normal to the smectic layer plane (x - y plane), with a magnitude depending on the layer spacing d ($|\vec{q}| = 2\pi/d$). Moreover, we assume that the director \vec{n} is fixed at the z - x plane for convenience. Considering the Cartesian coordinate system where the z axis is parallel to \vec{q} , the orientation of the molecular long axis \vec{a} is defined in terms of polar and azimuthal angles θ and ϕ , respectively. Besides, the orientation of molecular long axis in relation to the director is represented by the angle ψ , which satisfies the relation

$$\cos \psi = \cos \theta \cos \omega + \sin \theta \sin \omega \sin \phi. \quad (1)$$

In what follows, we assume that the average tilt direction is the same for all smectic layers and the molecular centers are randomly distributed inside the smectic layers. Furthermore,

we consider that a nonnull average tilt leads to a contraction of the layer spacing, being defined by $d = d_0 \cos \omega$, with d_0 denoting the layer spacing in the Sm-A phase, as represented in Fig. 1(b).

Using Govind and Madhusudana's approach [33,34], we consider a single-particle mean-field potential that corresponds to an extension of McMillan's model with the inclusion of a tilting term, written as

$$V = -V_0 \left\{ \left[s + \alpha \sigma \cos \left(\frac{2\pi z}{d} \right) \right] P_2(\cos \psi) + \alpha \beta \sigma^2 \eta \sin 2\theta \cos \phi \right\}. \quad (2)$$

In Eq. (2), V_0 is a typical interaction energy that determines the scale of the nematic-isotropic transition temperature of bulk sample; $P_2(\cos \psi)$ is the second-order Legendre polynomial, with ψ being the angle between the molecular long axis and the director \bar{n} ; s , σ and η are orientational, translational and tilt-order parameters, respectively, and β is a constant associated with the geometrical arrangement and amplitude of the dipoles in rodlike molecules. The quantity α is given by

$$\alpha = 2 \left(\frac{\alpha_0}{2} \right)^{\sec^2 \omega}, \quad (3)$$

in which α_0 is the geometric parameter related to the length of alkyl chains of rodlike molecules, through the expression $\alpha_0 = 2 \exp[-(\pi r_0/d)^2]$, with r_0 being a characteristic length associated with the molecular rigid part.

The order parameters s , σ , and η are defined by

$$s = \langle P_2(\cos \psi) \rangle, \quad (4)$$

$$\sigma = \langle P_2(\cos \psi) \cos(2\pi z/d) \rangle, \quad (5)$$

and

$$\eta = \langle \sin(2\theta) \cos \phi \rangle. \quad (6)$$

The thermodynamical averages, $\langle \dots \rangle$, are computed from the one-particle distribution function, that is,

$$\mathcal{Z}(z, \theta, \phi) \propto \exp[-V/k_B T], \quad (7)$$

in which k_B is the Boltzmann constant and T is the temperature. The equilibrium order parameters are solutions of the self-consistent equations, corresponding to the extreme values of the Helmholtz free energy, given by

$$\frac{F}{N_0 V_0} = \frac{1}{2} (s^2 + \alpha \sigma^2 + \alpha \beta \sigma^2 \eta^2) - \frac{k_B T}{V_0} \ln \left[\frac{1}{2\pi d} \int_{-1}^1 d \cos(\theta) \int_0^\pi d\phi \int_0^d dz \mathcal{Z} \right], \quad (8)$$

where N_0 is the number of molecules. The equilibrium state is determined from the global minimum of the Helmholtz free energy. The solutions corresponding to the different phases are

- (1) $s = \sigma = \eta = 0 \rightarrow$ Isotropic;
- (2) $s \neq 0$ and $\sigma = \eta = 0 \rightarrow$ Nematic;
- (3) $s \neq 0$, $\sigma \neq 0$ and $\eta = 0 \rightarrow$ Sm-A;
- (4) $s \neq 0$, $\sigma \neq 0$ and $\eta \neq 0 \rightarrow$ Sm-C.

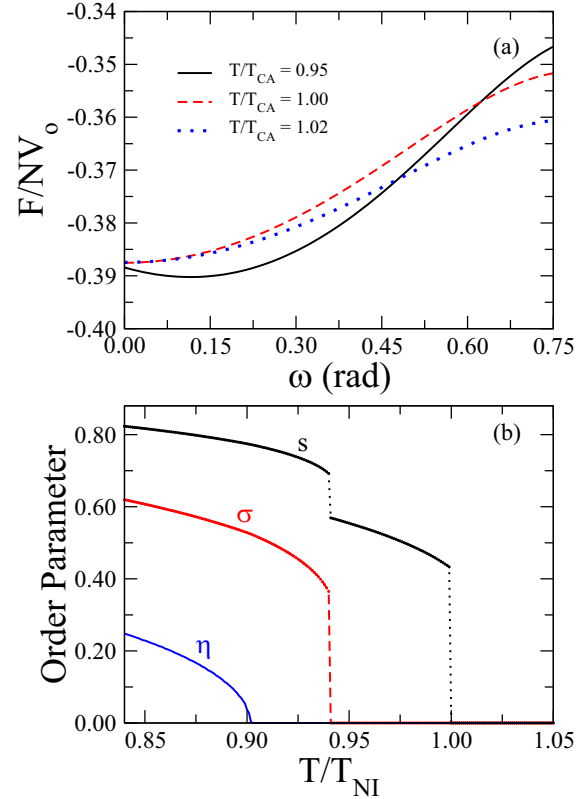


FIG. 2. (a) Helmholtz free energy as a function of the tilt angle ω , at the vicinity of the Sm-C–Sm-A transition temperature, T_{CA} . We use representative values of the model parameters: $\alpha_0 = 0.85$ and $\beta = 0.33$. Notice that a nonnull tilt angle corresponds to a minimum of the Helmholtz free energy for $T < T_{CA}$. (b) Temperature dependence of tilt, η , translational, σ , and orientational, s , order parameters for $\alpha_0 = 0.85$ and $\beta = 0.33$. We observe that η decays continuously as the system temperature is increased, while σ and s stay finite, signaling a second-order Sm-C–Sm-A phase transition.

In the present model, the order parameters are numerically determined using the self-consistent equations for different values of the tilt angle ω , for fixed values of T , α_0 , and β . The equilibrium configuration is determined from the minimum value of the Helmholtz free energy with respect to ω .

In Fig. 2(a), we present the Helmholtz free energy as a function of the average tilt angle, at the vicinity of the Sm-C–Sm-A transition temperature, T_{CA} . We consider as representative values of the model parameters $\alpha_0 = 0.85$ and $\beta = 0.33$. For $T > T_{CA}$, we notice that the null tilt angle corresponds to the only minimum of the Helmholtz free energy, which excludes the possibility of a coexistence of Sm-C and Sm-A phases at $T = T_{CA}$. Such a scenario is typical of a second-order phase transition, where the energy minimum in the disordered phase becomes a local maximum in the ordered one. In fact, a nonnull value of the tilt angle becomes the minimum of the Helmholtz free energy when $T < T_{CA}$. In Fig. 2(b), we show the temperature dependence of s , σ and η order parameters. The system temperature is normalized by the nematic-isotropic transition temperature, $T_{NI} = 0.2202V_0/k_B$. The tilt-order parameter η decays continuously as the system temperature is raised, while the

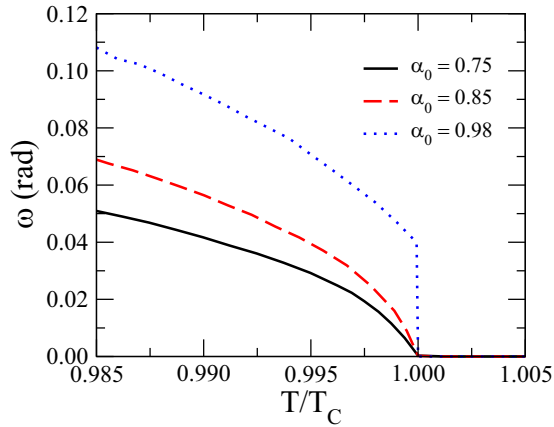


FIG. 3. The tilt angle as a function of T/T_C for $\beta = 0.33$ and three representative values of the geometric parameter α_0 : $\alpha_0 = 0.75$ (black solid line), $\alpha_0 = 0.85$ (red dashed line), and $\alpha_0 = 0.98$ (blue dotted line), where T_C represents the temperature where η order parameter vanishes. Notice that the continuous decay of the tilt angle is replaced by a discontinuous behavior as the parameter α_0 is increased.

orientational- and translational-order parameters stay finite, characterizing a second-order Sm-C–Sm-A phase transition at $T/T_{NI} = 0.902$. For $\eta = 0$, the single-particle potential is reduced to that of McMillan’s model, which predicts that a first-order Sm-A–N phase transition takes place for $\alpha_0 > 0.70$. We notice that the translational-order parameter σ develops a discontinuity at $T/T_{NI} = 0.941$, which is accompanied by an abrupt reduction of the orientational order parameter s , signaling a first-order Sm-A–N phase transition. Moreover, we can use T_{CA}/T_{NI} and T_{AN}/T_{NI} ratios to compare the present results with experimental findings for smectogenic compounds with a small transverse dipole moment. We recall that the nonchiral liquid-crystalline compound p-decyloxybenzoic acid p-n-hexyphenyl ester (DOBHOP) exhibits a second-order Sm-C–Sm-A phase transition, followed by a first-order Sm-A–N phase transition, with $T_{CA}/T_{NI} = 0.872$ and $T_{AN}/T_{NI} = 0.937$ [47]. As the DOBHOP molecules present a small transverse dipole moment ($P \approx 4$ nC/cm²) [48], the present results indicate that the single-particle molecular potential of Eq. (2) provides a reasonable description of the phase sequence of DOBHOP compound, with $\alpha_0 = 0.85$ and $\beta = 0.33$.

To characterize the effects of molecular structure on the tilt behavior of Sm-C phase, we analyze the temperature dependence of tilt angle for $\beta = 0.33$ and distinct values of the parameter α_0 , as shown in Fig. 3. For the sake of convenience, the system temperature was rescaled by T_C , which corresponds to the temperature at which the η order parameter vanishes. As the parameter α_0 is increased, we observe that the continuous decay of the tilt angle is replaced by a discontinuous jump at $T = T_C$. Such a behavior suggests that the value of the parameter α_0 affects the nature of the phase transitions involving Sm-C phase, even though β is kept constant. Since α_0 is associated with the length of alkyl-chain in rodlike molecules, this result is in agreement with experimental findings for different homologous series [20,49], where the molecular rigid part is kept constant and the length of alkyl-chain is varied. For $T < T_C$, we notice that the tilt

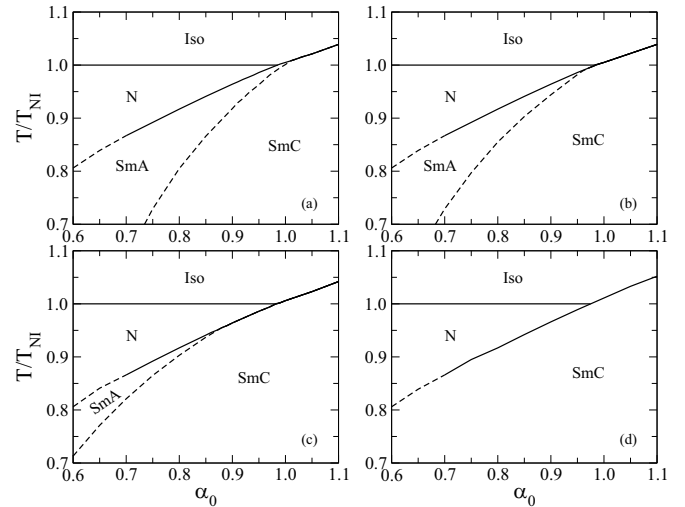


FIG. 4. The phase diagram in the reduced temperature vs α_0 plane for different values of the parameter β . (a) $\beta = 0.30$, (b) $\beta = 0.33$, (c) $\beta = 0.40$, and (d) $\beta = 0.70$. Solid (dotted) lines corresponds to first-order (second-order) transitions. As the parameter β increases, the Sm-A phase disappears.

angle is favored as the value of the parameter α_0 is raised, with the layer contraction becoming more pronounced.

In Fig. 4, we present the phase diagrams, temperature versus the parameter α_0 , considering different values for the parameter β . The temperature is rescaled by nematic-isotropic transition temperature, T_{NI} . For $\beta = 0.30$, we observe a second-order Sm-C–Sm-A phase transition for $\alpha_0 < 1.01$, while a first-order Sm-C–Iso phase transition takes place for $\alpha_0 > 1.01$, as shown in Fig. 4(a). This indicates that $\alpha_0 = 1.01$ is a critical end point, which corresponds to the position where the line of continuous Sm-C–Sm-A transition encounters the coexistence line between the Sm-C and the isotropic phase. Similar to McMillan’s model [50], we observe a tricritical point at $\alpha_0 = 0.70$, delimiting the regions of continuous and discontinuous Sm-A–N transitions. Moreover, one can note the triple point at $\alpha_0 = 0.98$, which determines the coexistence of nematic, Sm-A and isotropic phases. This phase behavior is in agreement with experimental findings for terephthal-bis-(4n)-alkylaniline (TBnA) [20] and 2-(4-alkyloxyphenyl)-5-alkyloxypyrimidines (PhPn) [49] homologous series. In Fig. 4(b), we show the T - α_0 phase diagram for $\beta = 0.33$, where a critical end point is observed for $\alpha_0 = 0.96$. However, the line of continuous Sm-C–Sm-A transition reaches the coexistence line of discontinuous Sm-A–N transition, thus corresponding to a N–Sm-A–Sm-C critical end point. A similar scenario is observed for $\beta = 0.40$, as presented in Fig. 4(c). It is remarkable that the N–Sm-A–Sm-C critical end point is displaced to lower values of α_0 as β is increased, which is accompanied by a reduction in the Sm-A temperature range. For $\beta = 0.70$, the Sm-A phase is suppressed and a tricritical point at $\alpha_0 = 0.70$ delimits the regions of continuous and discontinuous Sm-C–N transitions, as shown in Fig. 4(d). We notice that the NA tricritical point and the N–Sm-A–Sm-C critical end point tend to merge as the parameter β is increased, thus giving rise to a NC tricritical point. It is important to emphasize that

the Sm-A phase is stabilized by the layer contraction, without the need to introduce an excluded-volume contribution, as suggested by Govind and Madhusudana [33,34]. In this case, the single-particle mean-field potential introduced in Eq. (2) captures the main features of the phase transitions involving Sm-C phase, with a reduced number of free parameters.

III. EXTENDED MOLECULAR MODEL FOR FREE-STANDING FILMS

Let us now describe phase transitions in free-standing Sm-C films. We consider an extended version of McMillan-Mirantsev's model [51], by inserting the effective tilting potential. We assume a stratified film with N discrete layers, where each layer has its own set of orientational, s_i , translational, σ_i , and tilt, η_i , order parameters. Considering the layer located at the position z_i and the molecular orientation defined by polar and azimuthal angles, θ_i and ϕ_i , respectively, the effective one-particle mean-field potential can be written as

$$V_i = -V_0 \{ P_2(\cos \psi_i) [\bar{s}_i + \alpha_i \bar{\sigma}_i \cos(2\pi z_i/d_i)] + \alpha_i \beta \bar{\sigma}_i^2 \bar{\eta}_i \sin(2\theta_i) \cos \phi_i \}, \quad (9)$$

in which $\alpha_i = 2(\alpha_0/2)^{\sec^2 \omega_i}$, $d_i = d_0 \cos \omega_i$, and ω_i is the tilt angle in the i th layer, satisfying the angular relation $\cos \psi_i = \cos \theta_i \cos \omega_i + \sin \theta_i \sin \omega_i \sin \phi_i$. In addition, \bar{s}_i , $\bar{\sigma}_i$, and $\bar{\eta}_i$ are the average order parameters in i th layer and its two neighboring layers, being given by

$$\bar{s}_i = \frac{(1 - \delta_{i-1,0})s_{i-1} + s_i + (1 - \delta_{i+1,N+1})s_{i+1} + \frac{W_0(\delta_{i,1} + \delta_{i,N})}{V_0}}{3}, \quad (10)$$

$$\bar{\sigma}_i = \frac{(1 - \delta_{i-1,0})\sigma_{i-1} + \sigma_i + (1 - \delta_{i+1,N+1})\sigma_{i+1}}{3}, \quad (11)$$

and

$$\bar{\eta}_i = \frac{(1 - \delta_{i-1,0})\eta_{i-1} + \eta_i + (1 - \delta_{i+1,N+1})\eta_{i+1}}{3}, \quad (12)$$

with $i = 1, 2, \dots, N$, and δ_{ij} is the Kronecker's δ . In this approach, the surface anchoring is represented by a surface orientational field of strength W_0 . For free-standing Sm-C film, we assume that the surface ordering gives rise to a tilt angle profile as follows [52]:

$$\omega_i = \omega_B + \frac{(\omega_S - \omega_B) \cosh [d_0(2i - N - 1)/2\xi]}{\cosh [d_0(N - 1)/2\xi]}, \quad (13)$$

where ω_B is the bulk tilt angle and ω_S is the tilt angle in outermost layers. ξ is the surface penetration length, which delimits the range of anchoring effects on the tilt ordering along the film. As we consider a short-range surface contribution in the one-particle mean-field potential, we assume $\xi = 2d_0$. In fact, previous studies reported that the surface penetration length is of the order of the average smectic layer spacing d_0 [45,53,54], not exceeding a few molecular layers. It is important to highlight that the tilt angle profile defined by Eq. (13) was introduced by Tweet and co-workers [52], using a simple phenomenological elastic model. However, experimental results indicate that the tilt angle disappears before the layered structure is disrupted when the film temperature is

increased [21,55,56]. To provide a better description of free-standing Sm-C films, we consider that the surface tilt angle presents a typical temperature dependence of a mean-field model, that is,

$$\omega_S = \omega_0 \left(\frac{T_{AN} - T}{T_{AN} - T_{CA}} \right)^{\frac{1}{2}}. \quad (14)$$

In Eq. (14), T_{CA} and T_{AN} are the bulk Sm-C–Sm-A and Sm-A–N transition temperatures, respectively. In this model, ω_S vanishes as the smectic order is reduced. In what follows, we use $\omega_0 = 0.26$ ($\sim 15^\circ$).

The local order parameters s_i , σ_i , and η_i are defined as the thermodynamical averages

$$s_i = \langle P_2(\cos \psi_i) \rangle, \quad (15)$$

$$\sigma_i = \langle P_2(\cos \psi_i) \cos(2\pi z_i/d_i) \rangle, \quad (16)$$

and

$$\eta_i = \langle \sin(2\theta_i) \cos \phi_i \rangle, \quad (17)$$

being computed from the one-particle distribution function in the i th smectic layer, that is,

$$\mathcal{Z}_i \propto \exp[-V_i/k_B T]. \quad (18)$$

The total Helmholtz free energy is then given by

$$\frac{F}{N_0 V_0} = \sum_{i=1}^N F_i, \quad (19)$$

with

$$F_i = \frac{1}{2} (s_i \bar{s}_i + \alpha_i \sigma_i \bar{\sigma}_i + \alpha_i \beta \bar{\sigma}_i^2 \bar{\eta}_i) - \frac{k_B T}{V_0} \ln \left[\frac{1}{2\pi d_i} \int_{-1}^1 d \cos(\theta_i) \int_0^\pi d \phi_i \int_{(i-1)d_{i-1}}^{i d_i} dz_i \mathcal{Z}_i \right]. \quad (20)$$

From this model, we can compute the profile of the order parameters for different sets of free parameters in the single-particle mean-field potential: α_0 , β , and W_0 . Indeed, we use the tilt angle profile defined in Eq. (13) to obtain the actual profiles of order parameters that minimize the Helmholtz free energy, thus yielding the equilibrium configuration of the system. It is important to highlight that the tilt angle profile of Eq. (13) has been widely used in several experimental studies, leading to a reasonable description of the thermal and hydrodynamic properties of free-standing Sm-C films [28,52,55].

In combination with Eq. (14), we use the bulk values of ω_B to compute the tilt angle profile for distinct film temperatures, as shown in Fig. 5. We consider $N = 15$, $\omega_0 = 0.26$, $\alpha_0 = 0.85$, and $\beta = 0.33$. We observe that Eq. (13) provides a tilt profile with a positive curvature, where the outermost layers present tilt angles larger than the internal ones. For $T > T_{CA}$, a pronounced tilt reduction takes place at central layers as ω_B vanishes, while a non vanishing tilt persists in outermost layers. Such a scenario is similar to the experimental findings, where the surface layers exhibit a Sm-C–Sm-A transition well above the bulk transition temperature [21]. Besides, it

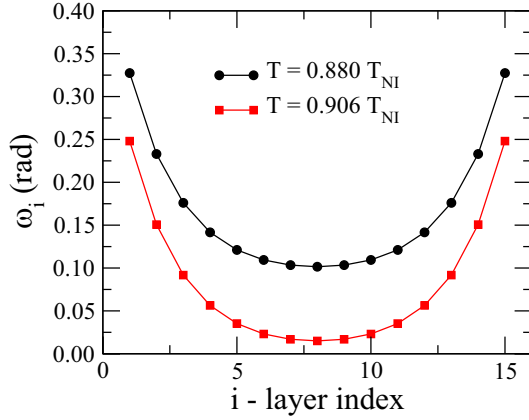


FIG. 5. Tilt angle profile for a $N = 15$ layer film, for distinct temperatures: $T = 0.880T_{NI}$ (black circles) and $T = 0.906T_{NI}$ (red squares). We consider $\omega_0 = 0.26$, $\alpha_0 = 0.85$, and $\beta = 0.33$. For these parameters, bulk Sm-C–Sm-A transition temperature is estimated as $T_{CA} = 0.902T_{NI}$. Notice that a pronounced reduction takes place in the tilt angle of central layers when $T > T_{CA}$, while a nonnull tilt persists in outermost layers.

is important to stress that the tilt angle profile is assumed to be independent of the surface anchoring, W_0 .

In Fig. 6, we present the profiles of order parameters for a free-standing smectic film with $N = 15$ layers. We use the same model parameters of Fig. 5. Furthermore, we consider $W_0/V_0 = 0.25$, which corresponds to the regime of weak surface anchoring [35]. For $T < T_{CA}$, we observe that nematic and smectic order parameters present nonuniform profiles with a negative curvature, where central layers are more ordered than the surface. More specifically, the weak anchoring leads to a small value of smectic order parameter in surface layers. However, the tilt-order parameter exhibits a nonuniform profile with a positive curvature. This profile is characterized by a high tilt ordering in surface layers, due to the tilt angle profile defined in Eq. (13). Such a scenario holds for $T > T_{CA}$, with a small reduction in the nematic and smectic order parameters. However, the tilt-order parameter becomes almost negligible in central layers, while surface layers present a finite tilt ordering. In this case, surface layers remain in the Sm-C phase, with the central layers being in the Sm-A phase. These results show that the tilt angle profile is the dominant effect in the regime of weak surface anchoring.

A distinct scenario emerges in the regime of strong surface anchoring, where profound modifications can be observed in the profiles of order parameters near the bulk Sm-C–Sm-A transition temperature, as exhibited in Fig. 7. Figure 7(a) shows that the profile of the nematic order parameter presents a positive curvature, with surface layers exhibiting an almost saturated orientational ordering. Such a behavior holds for $T > T_{CA}$, with a small reduction in the nematic order parameter of internal layers. In Fig. 7(b), we observe that the smectic order parameter exhibits a nonuniform profile with a negative curvature for $T < T_{CA}$. In this case, internal layers are more ordered than the outermost ones. For $T > T_{CA}$, the smectic order parameter exhibits a nearly flat profile, in which a small positive curvature can be verified. Although W_0/V_0 is not directly coupled to the tilt ordering, we notice that the

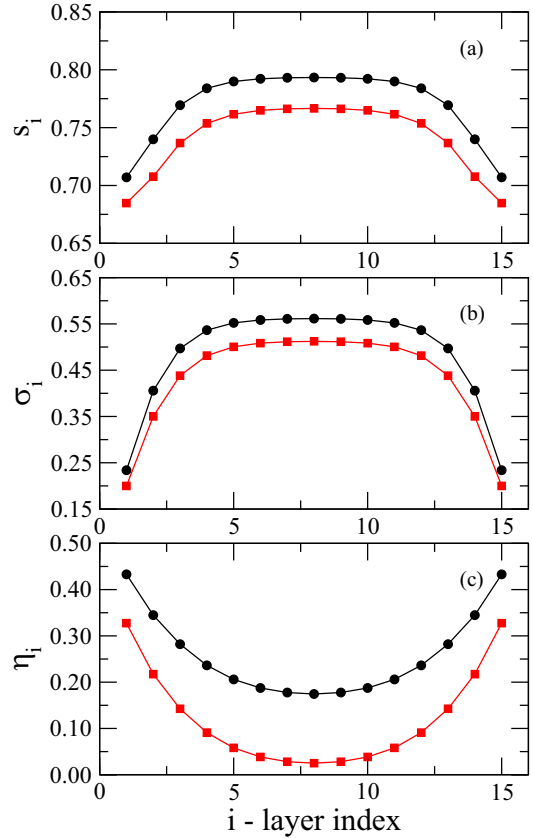


FIG. 6. Profiles of (a) orientational, (b) translational, and (c) tilt-order parameters for a free-standing film with $N = 15$, at different temperatures: $T = 0.880T_{NI}$ (black circles) and $T = 0.906T_{NI}$ (red squares). The model parameters are the same used in Fig. 5, where the bulk Sm-C–Sm-A transition temperature takes place at $T_{CA} = 0.902T_{NI}$. We use $W_0/V_0 = 0.25$, corresponding to the regime of weak anchoring condition. Notice that the tilt-order parameter stays finite in the surface layers above the bulk Sm-C–Sm-A transition temperature, even in the regime of weak surface anchoring.

strong anchoring condition leads to the enhancement of η_i along the whole film, specially in surface layers, as presented in Fig. 7(c). For $T > T_{CA}$, a strong surface anchoring tends to stabilize the tilt order along the film, with exception of the central layers where tilt ordering is negligible.

To investigate the interplay of finite size effects and surface anchoring conditions, in Fig. 8 we analyze the thickness dependence of order parameters at the central layer of free-standing films for distinct anchoring regimes. The penetration surface length is kept constant, with $\xi = 2d_0$. In the regime of weak surface anchoring, the nematic and smectic order parameters of central layer increase rapidly as the film thickness is enhanced, reaching their maximum values for $N = 15$. However, the tilt-order parameter exhibits a gradual reduction as the film thickness increases, thus reflecting the thickness dependence of tilt angle defined by Eq. (13). This result indicates that the finite size effects govern the thermal behavior of order parameters in the regime of weak surface anchoring. A distinct behavior is observed for strong surface anchoring, as shown in Fig. 8(b). The nematic order parameter at the central layer is independent of the film thickness, while

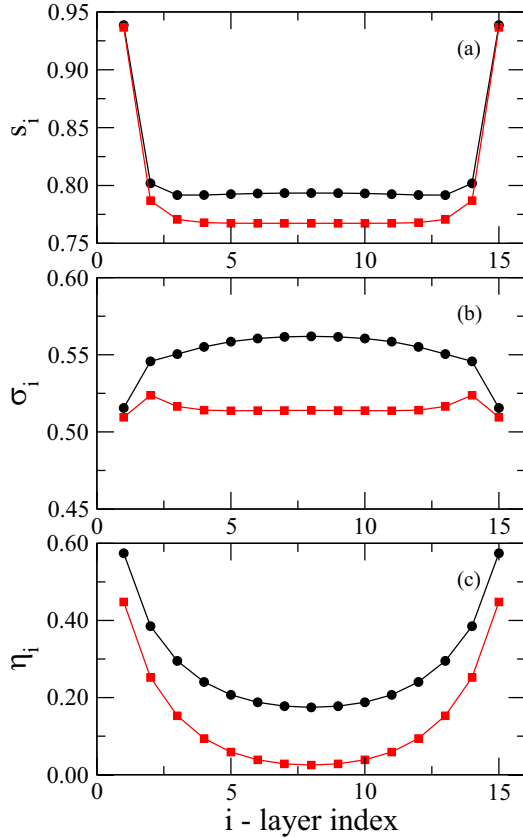


FIG. 7. Profiles of (a) orientational, (b) translational, and (c) tilt-order parameters for a free-standing smectic film, at the vicinity of bulk Sm-C–Sm-A transition temperature ($T_{CA} = 0.902T_{NI}$). We consider different film temperatures: $T = 0.880T_{NI}$ (black circles) and $T = 0.906T_{NI}$ (red squares). The model parameters are $\alpha_0 = 0.85$, $\beta = 0.33$, $\omega_0 = 0.26$, $N = 15$, and $W_0/V_0 = 2.5$. We notice an enhancement in the tilt-order parameter due to the strong anchoring condition.

a very small increase is observed in the smectic order parameter. Concerning the tilt-order parameter, we notice that η_{cl} is slightly larger in thin films due to the strong surface anchoring. However, the effects of tilt angle profile predominates as the film thickness is increased. In fact, we have assumed that the surface tilt amplitude ω_0 is independent of the surface anchoring W_0 , as it is related to the molecular structure and excluded-volume contribution. More specifically, there is no experimental evidence supporting the dependence of surface tilt angle on the surrounding gas in free-standing films.

Figure 9 exhibits the temperature dependence of the order parameters at the central layer for different values of surface anchoring ($W_0/V_0 = 0.25$ and $W_0/V_0 = 2.5$) and two representative film thicknesses ($N = 7$ and $N = 25$). For a thin film with $N = 7$, we observe that a first-order Sm-C–N transition takes place in the regime of weak anchoring conditions, while the nematic order vanishes smoothly as the temperature is raised, as shown in Fig. 9(a). This result indicates the absence of the nematic-isotropic transition, even for small values of the anchoring strength. However, the transition to the nematic phase leads in practice to the film thinning or to the film rupture. For a thin film with $N = 7$ and strong anchoring con-

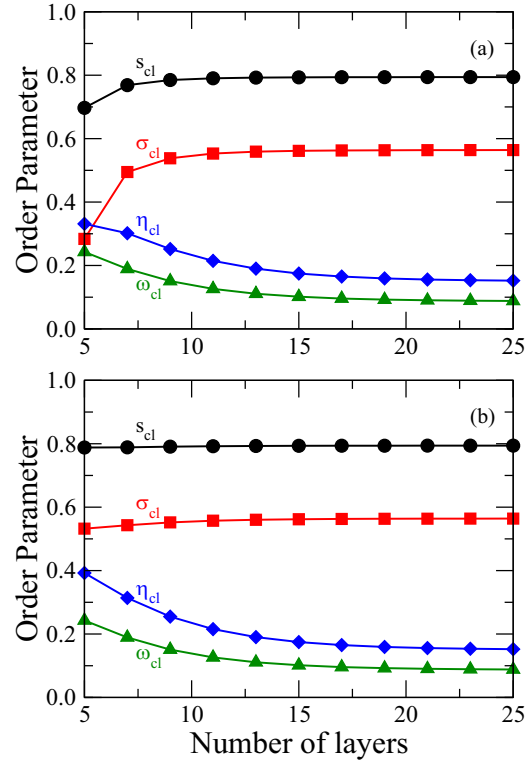


FIG. 8. Thickness dependence of order parameters in central layer of free-standing Sm-C films: nematic (s_{cl} , black circles), smectic (σ_{cl} , red squares), and tilt (η_{cl} , blue diamonds) order parameters. The tilt angle of central layer is also shown (ω_{cl} , green triangles). Different regimes of surface anchoring are considered: (a) $W_0 = 0.25$ and (b) $W_0 = 2.50$. The model parameters are $\alpha_0 = 0.85$, $\beta = 0.33$, and $\omega_0 = 0.26$. Notice that the surface anchoring plays an important role in central order parameters of thin films.

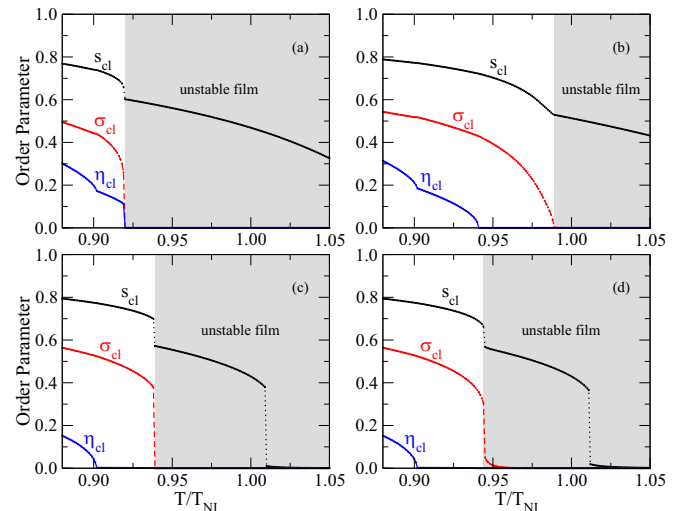


FIG. 9. Temperature dependence of order parameters at the central layer in smectic films with different thicknesses and anchoring conditions: (a) $N = 7$ and $W_0 = 0.25$, (b) $N = 7$ and $W_0 = 2.50$, (c) $N = 25$ and $W_0 = 0.25$, and (d) $N = 25$ and $W_0 = 2.50$. Notice that the interplay of finite size effects and surface anchoring may change the phase diagram of free-standing films. The gray areas represent the temperature regions where a dramatic reduction in the smectic order takes place, corresponding to an unstable film.

ditions, one can note that the first-order Sm-C– N transition is replaced by a sequence of second-order Sm-C–Sm-A and Sm-A– N transitions, occurring in higher temperatures than that observed in bulk systems [see Fig. 2(b)]. For the thicker film ($N = 25$), we observe a phase sequence similar to the bulk system, even for a weak anchoring strength, as observed in Fig. 9(c). Nevertheless, a residual smectic order parameter persists after the jump in Sm-A– N transition temperature for a 25-layer film under strong anchoring, as shown in Fig. 9(d). In this case, the nematic phase presents a residual smectic order, corresponding to a surface-induced smectic phase (si-Sm-A). A similar behavior is observed above the nematic-isotropic transition temperature, where a residual nematic order is observed.

IV. SUMMARY AND CONCLUSIONS

In summary, we have studied the phase transitions in bulk systems and free-standing films presenting a Sm-C phase. Using a single-particle mean-field potential introduced by Govind and Madhusudana [33], we have shown that the phase diagram of smectogenic compounds with a small transverse dipole can be reasonably described when the tilt-induced contraction of smectic layers is considered. This approach eliminates the need to introduce an additional excluded-volume contribution to stabilize the Sm-A phase, thus reducing the number of free parameters of the model. By varying the model parameter associated with the transverse dipoles in rodlike molecules, a rich variety of phase diagrams have been observed. In particular, we have identified a N –Sm-A–Sm-C critical end point, corresponding to the position at which the line of continuous transition between the Sm-C and Sm-A phases encounters the coexistence line between the Sm-C and the nematic phases. Concerning free-standing Sm-C films, our results showed that the interplay of finite size effects and surface anchoring conditions affects the phase diagrams of thin films. Considering a tilt angle profile and a discrete ver-

sion of single-particle mean-field potential, we have computed the profiles of order parameters of free-standing films under different anchoring regimes. We have observed that surface effects stabilize the tilt-order parameter in outermost layers of films above the bulk Sm-C–Sm-A transition temperature. As a consequence, surface layers may remain in the Sm-C phase, while the central layers are in the -Sm-A phase. Such a coexistence of Sm-C and -Sm-A phases in a free-standing film has been reported in previous experimental studies [24,46]. However, some questions still remain open, such as the possible connection between the surface anchoring strength and surface tilt angle. From a practical point of view, the control of the anchoring strength may be a challenging task. Although free-standing smectic films under strong anchoring condition have been widely probed, the scenario of films with a weak anchoring is very difficult to be realized. However, recent studies of free-standing smectic films immersed in aqueous solutions of surfactants revealed a reduction of anisotropic contribution of the surface tension [57,58], indicating a reduction of the orientational order at the surface layers. Furthermore, the effective control of surface anchoring has been realized in the study of spherical smectic shells [59], where an aqueous solution of an amphiphilic triblock copolymer was used to induce a weak homeotropic anchoring. Considering the status of the experiments nowadays, the present results may stimulate experimental efforts aiming to probe the rich scenario predicted by the extended version of the molecular theory for Sm-C liquid crystals.

ACKNOWLEDGMENTS

We are grateful to M. L. Lyra for useful discussions. This work was partially supported by Instituto Nacional de Ciência e Tecnologia de Fluidos Complexos (INCT-FCX), CAPES, CNPq/MCT, FAPEAL, and FINEP (Brazilian Research Agencies). I. N. de Oliveira thanks CNPq for the financial support (Grant No. 438198/2018-2).

-
- [1] C. W. Garland and G. Nounesis, *Phys. Rev. E* **49**, 2964 (1994).
 - [2] J. Morikawa, T. Hashimoto, A. Kishi, Y. Shinoda, K. Ema, and H. Takezoe, *Phys. Rev. E* **87**, 022501 (2013).
 - [3] J. Als-Nielsen, F. Christensen, and P. S. Pershan, *Phys. Rev. Lett.* **48**, 1107 (1982).
 - [4] T. Jin, G. P. Crawford, R. J. Crawford, S. Zumer, and D. Finotello, *Phys. Rev. Lett.* **90**, 015504 (2003).
 - [5] L. D. Pan, B. K. McCoy, S. Wang, W. Weissflog, and C. C. Huang, *Phys. Rev. Lett.* **105**, 117802 (2010).
 - [6] R. Geer, T. Stoebe, and C. C. Huang, *Phys. Rev. B* **45**, 13055 (1992).
 - [7] C. Y. Chao, C. R. Lo, P. J. Wu, Y. H. Liu, D. R. Link, J. E. Maclennan, N. A. Clark, M. Veum, C. C. Huang, and J. T. Ho, *Phys. Rev. Lett.* **86**, 4048 (2001).
 - [8] Z. Li and O. D. Lavrentovich, *Phys. Rev. Lett.* **73**, 280 (1994).
 - [9] M. S. S. Pereira, M. L. Lyra, and I. N. de Oliveira, *Phys. Rev. Lett.* **103**, 177801 (2009).
 - [10] O. Francescangeli, F. Vita, F. Fauth, and E. T. Samulski, *Phys. Rev. Lett.* **107**, 207801 (2011).
 - [11] W. H. de Jeu, B. I. Ostrovskii, and A. N. Shalaginov, *Rev. Mod. Phys.* **75**, 181 (2003).
 - [12] R. Holyst, D. J. Tweet, and L. B. Sorensen, *Phys. Rev. Lett.* **65**, 2153 (1990).
 - [13] C. Bahr, *Int. J. Mod. Phys.* **8**, 3051 (1994).
 - [14] T. Stoebe, P. Mach, and C. C. Huang, *Phys. Rev. Lett.* **73**, 1384 (1994).
 - [15] F. Bougrioua, P. Cluzeau, P. Dolganov, G. Joly, H. T. Nguyen, and V. Dolganov, *Phys. Rev. Lett.* **95**, 027802 (2005).
 - [16] E. S. Pikina, B. I. Ostrovskii, and W. H. de Jeu, *Eur. Phys. J. E* **38**, 13 (2015).
 - [17] T. Stoebe, L. Reed, M. Veum, and C. C. Huang, *Phys. Rev. E* **54**, 1584 (1996).
 - [18] K. Ema and H. Yao, *Phys. Rev. E* **57**, 6677 (1998).
 - [19] Z. H. Nguyen, M. Atkinson, C. S. Park, J. Maclennan, M. Glaser, and N. Clark, *Phys. Rev. Lett.* **105**, 268304 (2010).
 - [20] S. Kumar, *Phys. Rev. A* **23**, 3207 (1981).
 - [21] S. Heinekamp, R. A. Pelcovits, E. Fontes, E. Y. Chen, R. Pindak, and R. B. Meyer, *Phys. Rev. Lett.* **52**, 1017 (1984).

- [22] C. C. Huang and J. M. Viner, *Phys. Rev. A* **25**, 3385 (1982).
- [23] R. Shashidhar, B. R. Ratna, and S. K. Prasad, *Phys. Rev. Lett.* **53**, 2141 (1984).
- [24] C.-Y. Chao, S. W. Hui, and J. T. Ho, *Phys. Rev. Lett.* **78**, 4962 (1997).
- [25] M. R. M, K. P. Zuhail, A. Roy, and S. Dhara, *Phys. Rev. E* **97**, 032702 (2018).
- [26] C. C. Huang and S. C. Lien, *Phys. Rev. A* **31**, 2621 (1985).
- [27] C. Bahr and D. Fliegner, *Phys. Rev. A* **46**, 7657 (1992).
- [28] L. Reed, T. Stoebe, and C. C. Huang, *Phys. Rev. E* **52**, R2157 (1995).
- [29] H. Y. Liu, C. C. Huang, T. Min, M. D. Wand, D. M. Walba, N. A. Clark, C. Bahr, and G. Heppke, *Phys. Rev. A* **40**, 6759 (1989).
- [30] D. Brisbin, D. L. Johnson, H. Fellner, and M. E. Neubert, *Phys. Rev. Lett.* **50**, 178 (1983).
- [31] R. G. Priest, *J. Chem. Phys.* **65**, 408 (1976).
- [32] F. Gießelmann and P. Zugenmaier, *Phys. Rev. E* **55**, 5613 (1997).
- [33] A. S. Govind and N. V. Madhusudana, *Europhys. Lett.* **55**, 505 (2001).
- [34] A. S. Govind and N. V. Madhusudana, *Eur. Phys. J. E* **9**, 107 (2002).
- [35] K. Saunders, *Phys. Rev. E* **77**, 061708 (2008).
- [36] M. Osipov and G. Pajak, *Phys. Rev. E* **85**, 021701 (2012).
- [37] G. Pajak and M. A. Osipov, *Phys. Rev. E* **88**, 012507 (2013).
- [38] A. V. Emelyanenko and A. R. Khokhlov, *J. Chem. Phys.* **142**, 204905 (2015).
- [39] B. W. van der Meer and G. Vertogen, *J. Phys. Colloq.* **40**, C3-222 (1979).
- [40] M. V. Gorkunov, M. A. Osipov, J. P. F. Lagerwall, and F. Giesselmann, *Phys. Rev. E* **76**, 051706 (2007).
- [41] M. V. Gorkunov and M. A. Osipov, *J. Phys.: Condens. Matter* **20**, 465101 (2008).
- [42] M. V. Gorkunov, F. Giesselmann, J. P. F. Lagerwall, T. J. Sluckin, and M. A. Osipov, *Phys. Rev. E* **75**, 060701(R) (2007).
- [43] V. K. Dolganov, E. I. Demikhov, R. Fouret, and C. Gors, *JETP* **84**, 522 (1997).
- [44] M. S. Spector, P. A. Heiney, J. Naciri, B. T. Weslowski, D. B. Holt, and R. Shashidhar, *Phys. Rev. E* **61**, 1579 (2000).
- [45] A. Fera, R. Opitz, W. H. de Jeu, B. I. Ostrovskii, D. Schlauf, and C. Bahr, *Phys. Rev. E* **64**, 021702 (2001).
- [46] I. Kraus, P. Pieranski, E. Demikhov, H. Stegemeyer, and J. Goodby, *Phys. Rev. E* **48**, 1916 (1993).
- [47] S. Pestov and V. Vill, *Physical Properties of Liquid Crystals* (Springer-Verlag, Berlin, 2003).
- [48] P. O. Andreeva, V. K. Dolganov, C. Gors, R. Fouret, and E. I. Kats, *JETP Lett.* **67**, 856 (1998).
- [49] N. Kapernaum, C. S. Hartley, J. C. Roberts, F. Schoerg, D. Krueerke, R. P. Lemieux, and F. Giesselmann, *ChemPhysChem* **11**, 2099 (2010).
- [50] W. L. McMillan, *Phys. Rev. A* **4**, 1238 (1971).
- [51] M. V. Mirantsev, *Phys. Lett. A* **205**, 412 (1995).
- [52] D. J. Tweet, R. Holyst, B. D. Swanson, H. Stragier, and L. B. Sorensen, *Phys. Rev. Lett.* **65**, 2157 (1990).
- [53] C. Bahr, C. J. Booth, D. Fliegner, and J. W. Goodby, *Phys. Rev. E* **52**, R4612 (1995).
- [54] J. V. Selinger and D. R. Nelson, *Phys. Rev. A* **37**, 1736 (1988).
- [55] P. O. Andreeva, V. K. Dolganov, C. Gors, R. Fouret, and E. I. Kats, *Phys. Rev. E* **59**, 4143 (1999).
- [56] D. Schlauf, C. Bahr, and C. C. Huang, *Phys. Rev. E* **55**, R4885 (1997).
- [57] Y. Iwashita, S. Herminghaus, R. Seemann, and C. Bahr, *Phys. Rev. E* **81**, 051709 (2010).
- [58] K. Harth and R. Stannarius, *Phys. Chem. Chem. Phys.* **15**, 7204 (2013).
- [59] H.-L. Liang, R. Zentel, P. Rudquist, and J. Lagerwall, *Soft Matter* **8**, 5443 (2012).